Computational Study on Spectral Properties of the Selected Pigments from Various Photosystems: Structure−Transition Energy Relationship

Zuzana Vokáčová and Jaroslav V. Burda*

Department of Chemical Physics and Optics, Faculty of Mathematics and Physics, Charles University, Ke Karlovu 3, 121 16 Prague 2, Czech Republic

Received: February 28, 2007; In Final Form: April 21, 2007

In this study, the most important kinds of pigments (chlorophylls, bacteriochlorophylls, phycobilins, and carotenoids) from various photosystems were explored. For the most stable conformations, electronic transitions were determined at the TDDFT/6-31+G(d) level with the B3PW91 functional and compared to measured spectra. The group of carotenoids was also investigated at the TDA/TDDFT level with the BLYP functional. The energies of Q_y transitions are systematically blue-shifted by about 50−100 nm in the case of (bacterio)-chlorophyll and pheophytin molecules. Nevertheless, the correct relative order of the Q lines among various chlorophyll types was obtained through comparison with experimental results. Much better agreement was obtained for the Soret band, for which the differences between calculated and measured transitions were at most 35 nm. In the case of phycobilins, the first transition line was estimated to be at lower frequencies (around 500 nm) with a very similar blue shift of about 100 nm from experimental values. The influence of anchoring cysteine side chain(s) was found to be marginal. A dominant effect of the linear polyene chain on the determined spectral lines was found in the case of carotenoids. Nevertheless, the impact of β-cycles and epoxy and keto groups is clearly visible as well. The high intensity of the first allowed transition matches different characters of the HOMO and LUMO. In the case of fucoxanthin, the TDA method also predicts the B_u^- state to lie below the $1B_u^+$ state. Because the shift of electron transitions is approximately proportional to the size of the π-conjugated system, the shift of the calculated transitions compared to experimental values is practically constant for the same excitations of (bacterio)chlorophyll and phycobilin molecules. However, this is not true for carotenoids, for which both the transition energy and the shift of the transition vary with the number of conjugated double bonds.

Introduction

Photosyntetic pigments represent the lifeblood of all photoauthotrophic organisms. There are basically three classes of photosynthetic pigments: (bacterio)chlorophylls, carotenoids, and the smaller but still important phycobilins.[1] These pigments have been studied for many years, and several investigators have been recognized with Nobel Prizes in the distant and even recent past for elucidating the importance of the subject. Despite the great effort devoted to this subject, there is still much room for further exploration. We decided to examine the electron transition spectra of individual structures and the relationship between structure and transition energy in the above-mentioned pigment classes.

Experimental electronic spectra of these compounds can be found in many papers, monographs,[2] and spectral encyclopedias.[3] Because this work has a computational character, we concentrate here mainly on the theoretical studies dealing with spectra predictions (or estimations) performed on the chosen pigments and their models, using measured spectra for comparison and approximate error estimation.

For (bacterio)chlorophylls, the very first calculations were performed by Gouterman and co-workers[4−6] on the porphyrin ring, introducing the four-orbital model. Following these initial efforts, many other researchers have performed calculations at various levels using different models frequently based on free-base porphyrin; see, for instance, refs 7−24. These calculations are usually used for method-testing purposes, and up to now, they have usually been too demanding for larger pigment molecules or their aggregates. The electronic spectra of chlorophyll *a* have been explored in many studies, including those of Hasegawa et al.,[25] who used the relatively high-accuracy SAC-CI (symmetry-adapted cluster-configuration interaction) method, and Parusel and Grime,[26] who compared chlorophyll *a* and pheophytin. The orientation of two porphyrin rings in a dimeric arrangement was investigated and compared with experimental data (Raman spectroscopy) by Jeong et al.[27]

Spectroscopic properties of some bacteriochlorophylls (*a*, *b*, *c*1−3, and *d*) were studied using a semiempirical approach by Linnato et al.[28,29] Later, they extended the explored systems to self-organized aggregates of bacteriochlorophylls[30] and the LH II antenna structure.[31] Cory et al.[32] determined semiempirically electronic excitations in larger aggregates of bacteriochlorophylls. Accurate TDDFT (time-dependent density functional theory) calculations of chlorophyll *a* and bacteriochlorophyll *b* spectra have been published by Sundholm.[33,34]

In the case of (bacterio)chlorophyll molecules, for a comparison with experimental data, we used measurements of absorption spectra,[35,36] circular dichroism,[37] and fluorescence and absorption spectra.[38,39]

Phycobilins belong to the second group of pigments that are present in photosynthetic complexes. Phycobilins are linear open-chain tetrapyrrole systems anchored in proteins. An

* Corresponding author. E-mail: burda@karlov.mff.cuni.cz.

10.1021/jp071639t CCC: $37.00
Published on Web 06/08/2007

interesting recent study[40] addressed the spectral characterization of phycoerythrin in combination with quantum chemical calculations. Another study investigated regulation of the absorbed excitation energy by chlorophyll and phycobilin. Their models are based on X-ray structures of PS I, PS II, and allophycocyanin.[41]

Carotenoids are the last family of photosynthetic pigments that we examine in this study. Molecular structures of selected carotenoids were previously calculated semiempirically (AM1) by Hashimoto et al.[42] The obtained structures were compared with geometries from X-ray crystallography. Similarly, in the work of Wang et al.,[43] structural characteristics and (stacking) stabilization energies were explored using the MP2 approach. The role of beta-carotene in the quenching of singlet oxygen was examined in a study[44] using the DFT method. Great effort has also been devoted to calculations of electronic spectra. In the study of He et al.,[45] the complete active space SCF (CASSCF) technique was employed on the low-lying excited states of the carotenoid rhodopin glucoside (RG). The results showed that the lowest triplet state energy of the RG is below 0.78 eV. The authors also found a significant blue shift of the energy of the second excited singlet state (S2) in this carotenoid under the influence of bacteriochlorophylls. In another work,[46] theoretical and experimental approaches were combined to demonstrate some correlations between AM1 calculations and NMR spectroscopy. A large number of studies on carotenoid spectra have been published by the Fleming group,[47−61] who used both experimental and theoretical tools. Their quantum chemical calculations were done in collaboration with the group of Head-Gordon.[62−64] In one recent studies,[60] TDDFT and TDA/TDDFT (Tamm−Dancoff approximation)[65] calculations were used for the exploration of the energy transfer from the S1 state of peridinin to chlorophyll in photosystem (PS) I.

Although the TDA cannot generally be considered superior to the full TDDFT method, in carotenoids, it performs better because of the fact that full TDDFT overestimates the interactions of close-lying states, as pointed in a study by Hirata and Head-Gordon.[65]

Failures of the TDDFT method applied to dimers of pigments from photosystems and their models have been published, e.g., by Dreuw et al.[66] The problem results from unphysical charge transfer, which generates low-lying "ghost states". A remedy was recently suggested by Cai et al.[67]

In the present study, a systematic determination of TDDFT electronic spectra was performed for the most common (bacterio)chlorophylls, phycobilins, and carotenoids. The main goal of this study was a comparison of pure electron transition energies of isolated (optimal gas-phase) structures without any influence of neighboring peptide molecules, other pigments, or solvation effects using the same method and basis set. In this way, all undesired shifts can be suppressed, and genuine characteristics of individual structures can be elucidated.

Computational Details

First, several conformers of each pigment were chosen to find a global minimum. A structural database [Protein Data Bank[68] (pdb)] was used to obtain appropriate initial structures.

This selection was important in the case of the various conformers of chlorophyll (types *a*, *b*, *c*1−3, *d*) and bacteriochlorophyll (types *a*, *b*, *c*, *d*, *e*, *g*), whose structures are presented in Figures 1 and 2, respectively. Usually, several arrangements were possible, and it was not completely clear which could be excluded based on an exploration of the structural database because the described conformations usually depend strongly on the corresponding biological environment. Also, several structures of a given (bacterio)chlorophyll type were found to have similar total energies. One of the rare exceptions, for which several high-resolution X-ray structures are available, is the molecule of chlorophyll *a*. Our model structures were adopted from 1DOP pdb structure. In all investigated (bacterio)-chlorophyll conformers, the phytyl chain was excluded from consideration. Instead, the methyl ester anchoring group was used in the models. This can be assumed to be a reasonable approximation, as it follows from our preliminary calculations as well as from other studies (e.g., ref 69). For the other chlorophyll types, the original chlorophyll *a* ligands were replaced by appropriate substituents to create the required models. In the determination of pheophytin *a*, the structure of chlorophyll *a* was taken as a starting point, with the Mg^{2+} cation substituted by two protons.

In the case of the phycobilin group, two representatives were considered, as shown in Figure 3. The initial structures were obtained from the Protein Data Bank.[68] Because phycobilins can adopt many spatial conformations, the crystallographic structure of phycocyanobilin was chosen as a starting point to preserve the biologically relevant arrangement of the pigment. The models of phycoerythrobilin originate from the same starting structure with replacement of the different substituents and reduction of the double bond between the C and D pyrrole rings. In the case of phycoerythrobilin, two forms were considered: anchored through a single covalent bond to the sulfur atom of cysteine side chain and/or with a pair of covalent bonds as depicted in Figure 3.

In the case of carotenoids, nine pigments were chosen; they are displayed in Figure 4. Selection of these pigments allows for clarification of the influence of different structural elements on spectral characteristics. The all-trans conformation was used for linear carbon chains. The other substituents (e.g., xanthophyll and β-cycles) were constructed according to the basic "hybridization" rules, and the lowest-energy conformers were chosen for subsequent analysis.

Because all of the conformers represent quite an extended set of large molecules, several subsequent geometry optimizations were performed, making the selected set of conformers gradually smaller. The lowest-energy structures were finally reoptimized at the B3PW91/6-31G(d) level of theory. For these molecules, absorption spectra were determined with time-dependent density functional theory (TDDFT) using the same functional and the 6-31+G(d) basis set. The B3PW91 functional and basis set were chosen on the basis of our previous calculations on free-based porphine systems.[70,71] The diffuse functions were found to be of key importance for the determination of electron transitions, as described in many other studies (e.g., refs 72 and 73).

All calculations were performed using the Gaussian 03 program package.

Pigment Isomers/Conformers. Many relevant structures were considered in the first optimization step (HF/3-21G). In the next step, reduced sets of conformers (usually fewer than five) were considered, and the lowest-energy structures were reoptimized at the B3PW91/6-31G(d) level.

In the case of chlorophyll *b*, a pair of conformers with cis and trans orientations of the C7═O carbonyl bond in the formaldehyde group with respect to the C8 site (for the atom numbering, see Figure 5) exhibits a small energy difference (about 1 kcal/mol). Global minimum of chlorophyll *b* represents conformer with the oxygen from the −COH group in a trans arrangement with respect to the C8 atom. In this orientation,

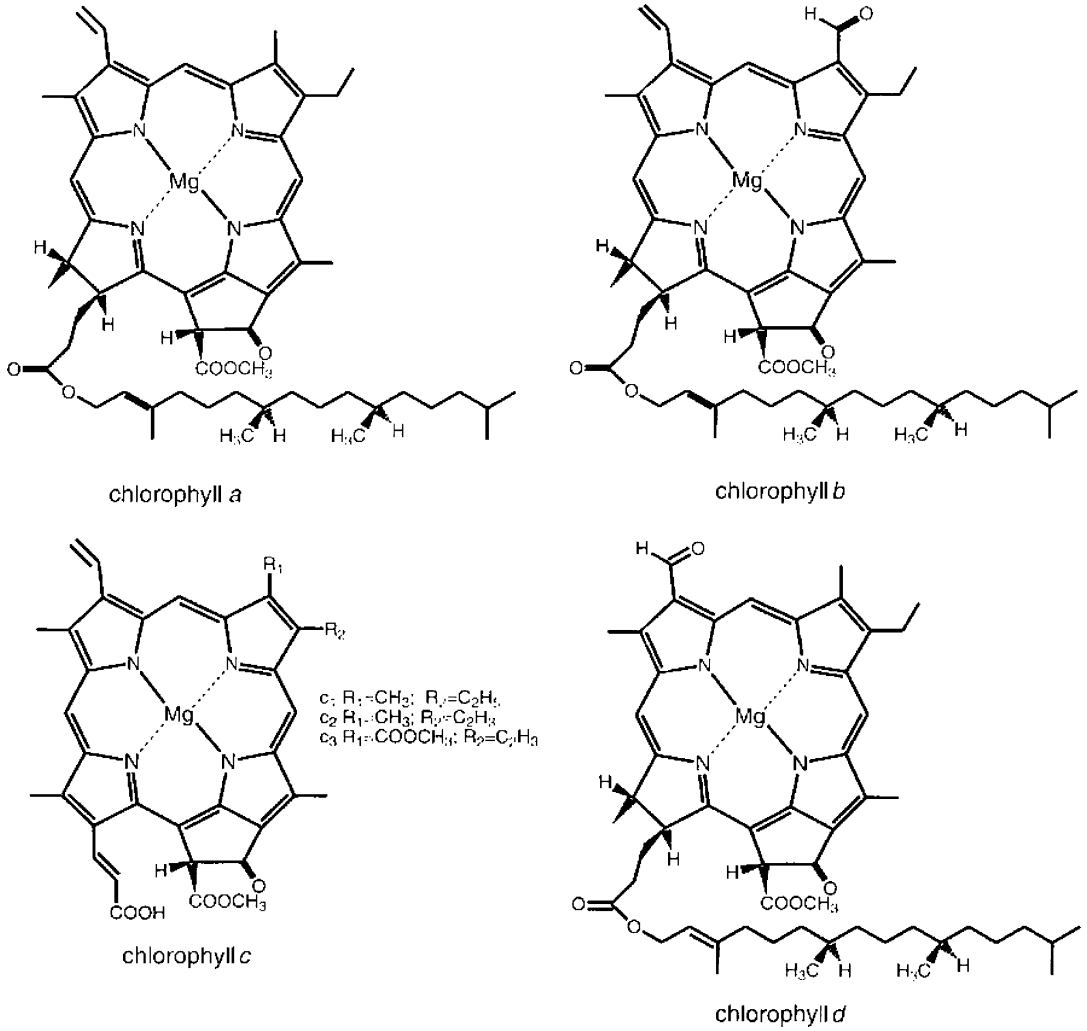

Figure 1. Structural formulas of the selected types of chlorophyll molecules.

the COH group is slightly less repelled by the surrounding protons and is better "incorporated" into the π-electron-conjugated system of the porphyrin ring. All lines in the spectrum of the cis conformer are mildly blue-shifted in comparison to those in the spectrum of the trans conformer (see Figure 6).

Electron Transition Spectra. For the global minima of the selected pigments, six electron singlet−singlet transitions were computed with the TDDFT method. In the discussion, usually three lines corresponding to visible (allowed) transitions are compared with experimental data. The full sets of transition lines are drawn in Figures 7−11 for chlorophyll molecules, bacteriochorophylls, pheophytin, bilins, and carotenoids, respectively. Numerical values together with intensities and experimental data are collected in Tables 1−4. In the case of carotenoids, it is known from many studies (for instance, refs 54, 63, 74, and 75) that the TDDFT approach does not give the correct order for the S1 and S2 states. Therefore, TDA methods (as implemented in Q-Chem 3.0[76]) were used with the same basis set and the non-hybrid functional BLYP.

Spectral characteristics

Chlorophylls. The spectra of chlorophyll molecules consist of two basic absorption bands. A most complex band, located in the blue region, is called the Soret band and is composed of several electron transitions. The other(s), called Q band(s), can usually be found in the red region. Their typical positions and intensities can be seen in the experimental spectra in Figure 12a. Such a distribution of electron transitions is responsible for the typical green or blue-green color of most chlorophyll pigments.

The calculated values of spectral lines are systematically blue-shifted in comparison to the experimental values by about 60−80 nm for the band Q_y and about 20−30 nm for the Q_x and Soret bands. Nevertheless, it is clear that a fairly good qualitative agreement with experimentally measured spectral lines has been obtained. In particular, the relative positions of spectral lines depending on various structural parameters (ligands) are in a very good accord with measured data for all chlorophyll types (both Chl and BChl).

Chlorophyll *a* is the most common chlorophyll pigment, and its spectrum is well established. The calculated values of the Q_y, Q_x, and B lines (B lines represent an edge of the Soret band) lie at 583, 539, and 398 nm, respectively. The measured intensity of the Q_y band (about 0.23) is in good accord with our results. However, we failed to reproduce the intensity of the Soret band of about 1.1 (similarly to some other researchers, e.g., ref 69). Nevertheless, in another measured spectrum (cf. Figure 12a), the intensities of both the Q_y and Soret bands are much closer to each other, in accord with our calculations.

From an analysis of molecular orbitals (MOs) and individual transitions it follows that the four-orbital model of Gouterman and co-workers can be still recognized as a reasonable approximation even within the TDDFT model. The first two transitions of chlorophylls (and also of bacteriochlorophylls and

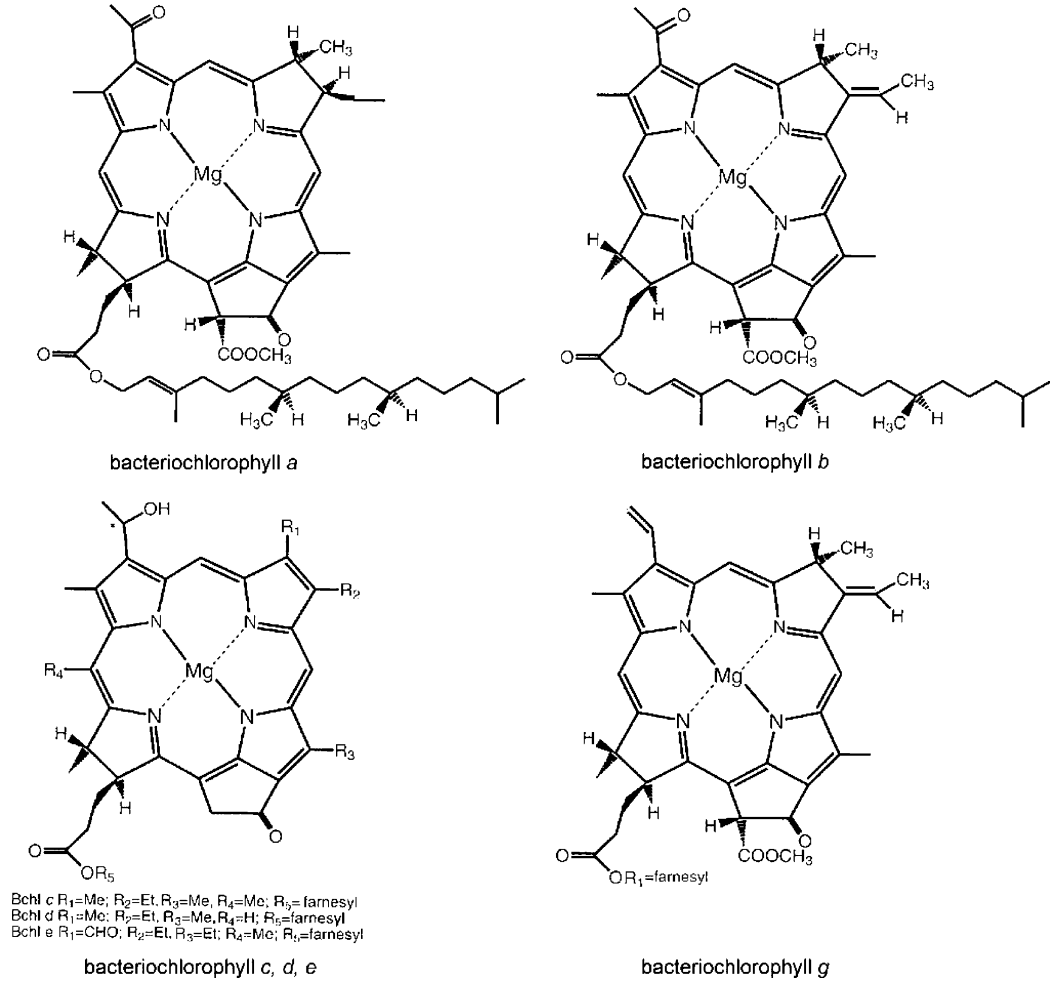

Figure 2. Structural formulas of the selected types of bacteriochlorophyll molecules.

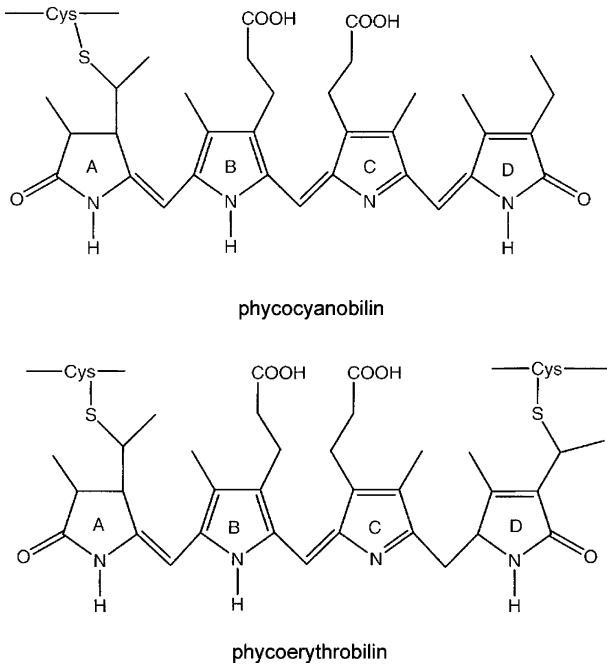

Figure 3. Structural formulas of the investigated phycobilins.

pheophytins) are always based primarily on these four MOs. The individual electron transitions can be compared with spectra of the Mg−porphin molecule.[70,71] It can be noticed that HOMO has features of the a_{1u} HOMO − 1 orbital in symmetrical Mg−porphin and, inversely, HOMO − 1 has the character of a_{2u} of the Mg−porphin HOMO (for the shapes of frontier orbitals, see Figure 13a−d). This can be generalized for all chlorophylls and bacteriochlorophylls with the exception of the Chl c family, in which the same order of frontier MOs as in Mg−porphin was found. However, these three systems have closer structural relationships to Mg−porphin than to the chlorin molecule (see below). Also, the near-degeneracy of the Mg−porphin HOMO and HOMO − 1 can be traced in the smallest energy difference of the HOMO and HOMO − 1 orbitals (less than 0.1 eV) in the case of chlorophyll *c*. The other frontier orbitals preserve the same character in all of the kinds of chlorophyll molecules considered herein. In structures without the D_{4h} symmetry of Mg−porphin, the LUMO and LUMO + 1 are no longer degenerate. This is in accord with the older theory, according to which such an MO crossing results from the removal of symmetry in passing from porphin to chlorin and bacteriochlorin models, as depicted in Figure 14. However, such a simple theory is not able to explain in detail the differences between individual types of chlorophylls and bacteriochlorophylls that are known from measured spectra and are computationally reproduced here.

Chlorophyll *b* differs from chlorophyll *a* in the C7 substituent group, where the methyl group of chlorophyll *a* is replaced by the formyl group.

In comparison with Chl a, a ligand variation causes a blue shift of the Q_y band of about 10 nm and a red shift of the Soret band of about 25 nm. From the orbital energies, it can be seen that the formyl group with the C═O double bond affects the conjugated system of chlorophyll *b*, decreasing the HOMO eigenvalue by about 0.3 eV. Otherwise, its character remains

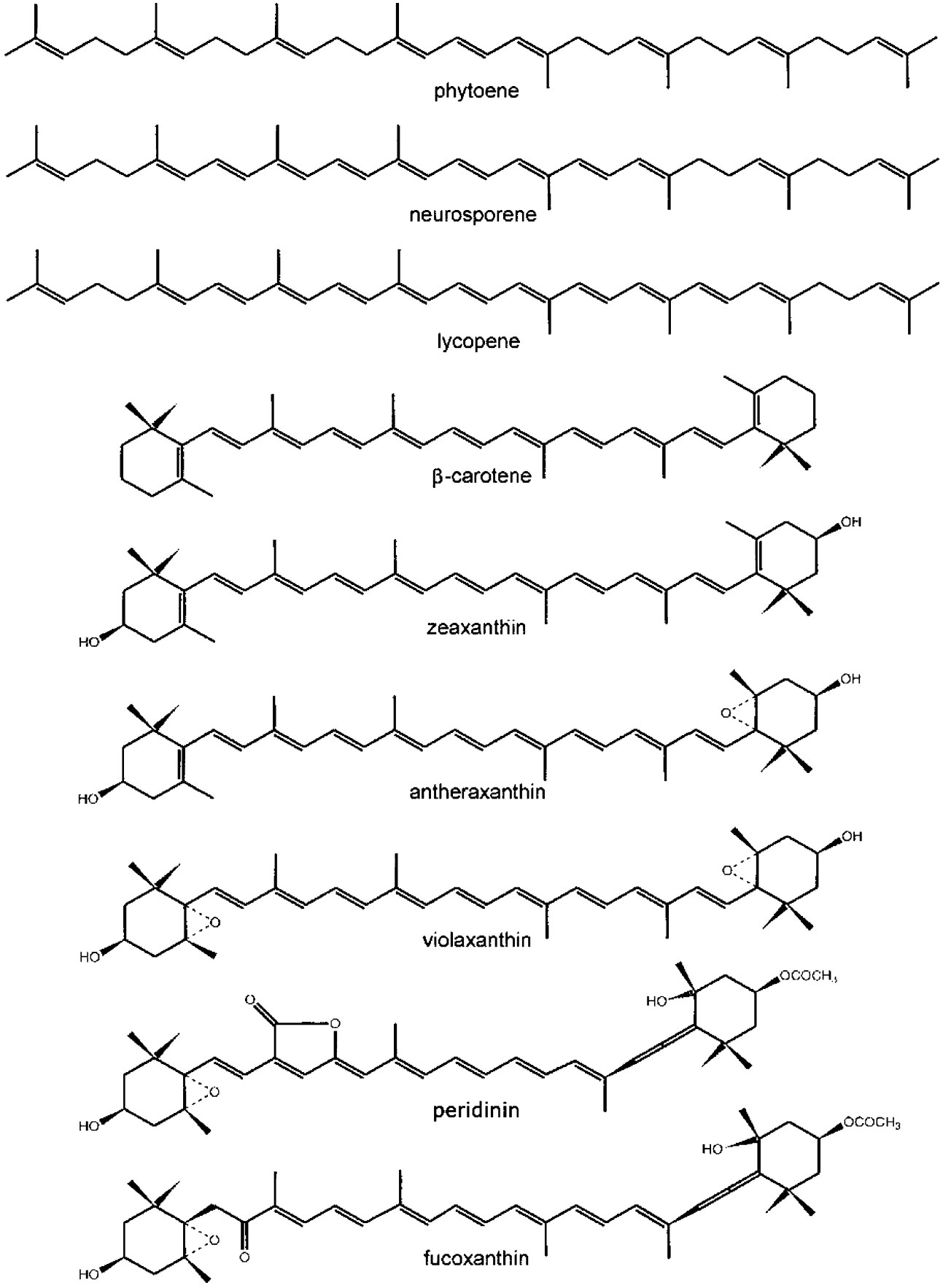

Figure 4. Structural formulas of the investigated carotenoids.

the same as in the Chl a molecule. However, the elongation of the π-conjugated system in the presence of the formyl group influences not only one MO. The −CHO group causes an energy shift of both the occupied and virtual frontier orbitals toward lower values, resulting in an actual blue shift of the first Q_y line with a reduced intensity. The red-shifted transitions in the

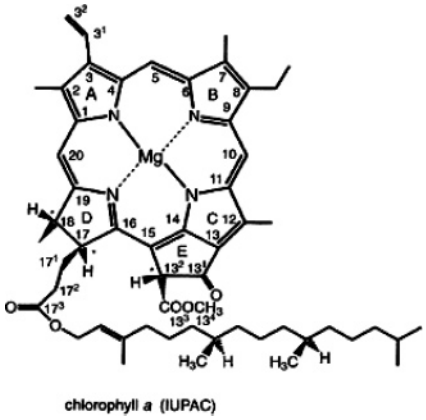

Figure 5. Chlorophyll *a*: atom numbering according to IUPAC conventions.

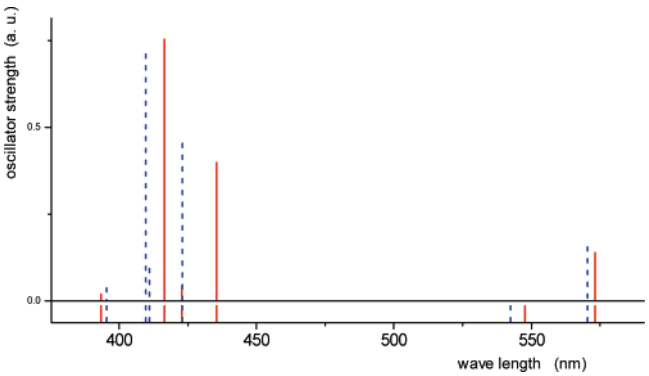

Figure 6. Lines of electron transitions of the chlorophyll *b* model molecules: positions of the COH group for the trans conformer (solid lines) and the cis conformer (dashed lines).

Soret band exhibit practically doubled intensities. The ratio of oscillator strengths of the Q_y band to the Soret band is markedly smaller for chlorophyll *b* than for chlorophyll *a*. This result is in very good agreement with the experimental data.[77] The analogous −CHO group is also present in bacteriochlorophyll *e*, displaying a similar blue shift of the Q_y band within the BChl c−e family.

Chlorophyll *c* molecules exhibit larger variability than the other chlorophylls. The isoprene tail, which is usually used for anchoring in the protein matrix, is not present. The pyrrole D ring is not reduced and thus the chlorophylls *c* more closely resemble the porphyrin system of the Mg−porphin molecule, whereas the other chlorophylls are derived from the chlorin system instead. This higher symmetry of the π-electron system explains why the spectral properties of chlorophylls *c* deviate from those of the other chlorophyll types. Also, as mentioned above, the order of the HOMO and HOMO − 1 corresponds to the electronic structure of Mg−porphin. These modifications of chlorophylls *c* substantially influence the spectral transitions. They are responsible for stronger absorption in the Soret band (390−440 nm) and a reduction of the two Q bands in the visible region above 500 nm. The Q_y band is substantially reduced, and its intensity is almost eliminated.

Mutual differences between chlorophylls *c* correspond to different substituents on carbons C7 and C8, as can be seen from Figure 1. Whereas types *c*1 and *c*2 exhibit the most blue-shifted Q_y band of all of the chlorophyll systems, both ligands of chlorophyll *c*3 have double bonds that interact with the π-electron system of the porphyrin ring, causing a visible red shift of the Q_y transition (by about 13 nm) in comparison to that of the *c*1 and *c*2 molecules. The energy of this spectral line is very similar to that of the Q_y line of chlorophyll *a*. The Q_x transition lies relatively very close to the Q_y band for all three structures, less than 10 nm. This is again a consequence of the higher symmetry of the porphyrin ring.

Chlorophyll *d* differs from chlorophyll *a* in the C3 position, where the formyl group is present instead of the vinyl group. In this way, chlorophyll *d* can be considered as an intermediate between chlorophyll *a* and bacteriochlorophyll *a* (in terms of both spectral transitions and structure). The Q absorption lines exhibit a larger red shift than in any other chlorophyll. This is the only chlorophyll with a calculated Q_y transition over 600 nm. The explanation lies in the fact that the formyl group influences all frontier orbitals (both occupied and virtual), shifting their orbital energies to lower values. In particular, the eigenvalue of the LUMO displays the lowest energy among the whole set of examined chlorophylls. The π orbital of the formyl group is incorporated into the π-conjugated system of the porphyrin (or chlorin) ring where an elongation of the appropriate lobe is clearly visible (cf. Figure 13e). The same effect of the formyl group can be also seen in the case of bacteriochlorophylls *a* and *b*.

Bacteriochlorophylls. The electronic spectra of the bacteriochlorophylls are depicted in Figure 8 and in Table 2. The basic structural difference between chlorophyll and bacteriochlorophyll groups lies in the reduced B and D pyrrole rings (whereas in chlorophylls, only the D ring is reduced). Therefore, bacteriochlorophylls have a more perturbed π-electron system than chlorophylls. This should seemingly lead to the absorption of light with shorter wavelengths. However, this conclusion is not completely correct because the consequences of the perturbed conjugated ring are not so simple and straightforward. Moreover, the shortening of wavelengths can be observed only in the case of the Soret band. In contrast, the Q_y band displays a red shift in accordance with the experimental spectrum (cf. Figure 12b). The explanation of this red shift can be sought in the fact that, in the HOMO − 1 (with a_{1u} character) of Mg−porphin, the p_z atomic orbitals (AOs) of carbons C7, C8, C17, and C18 (for atom numbering, see Figure 5) are involved. A reduction of these C7−C8 and C17−C18 bonds causes this MO to become increasingly less stable in passing to chlorin (or chlorophylls) and bacteriochlorin (or bacteriochlorophylls) (see Figure 14). Because the original HOMO (a_{2u}) of Mg−porphin is not affected by the reduction of the C−C bonds, the order of the HOMO and HOMO − 1 is exchanged in chlorophyll and bacteriochlorophyll molecules. Similarly, only one of the original e_g virtual orbitals contains the p_z AO of the same carbon atoms (C7, C8, C17, C18). Thus, only this virtual orbital is destabilized in an analogous manner. Therefore, the LUMO is practically unaffected, whereas the energy of the LUMO + 1 increases when a reduction of these two carbon bonds occurs (cf. Figure 14). This means that the gap between the HOMO and LUMO is actually smaller in bacteriochlorophyll than in chlorophyll systems, leading to Q_y absorption at longer wavelengths in bacteriochlorophylls.

It is interesting to notice that the position of the Q_x band is fairly stable, between 530 and 560 nm, regardless of whether chlorophylls, bacteriochlorophylls, or pheophytins are considered. Only the intensity is noticeably higher in the case of bacteriochlorophylls *a* and *b*.

All of the spectra of the bacteriochlorophylls calculated at the TD-B3PW91/6-31+G(d) level are collected in Figure 8. Generally, the computed transitions are blue-shifted from the measured absorption spectra, with an average shift of about 80 nm.

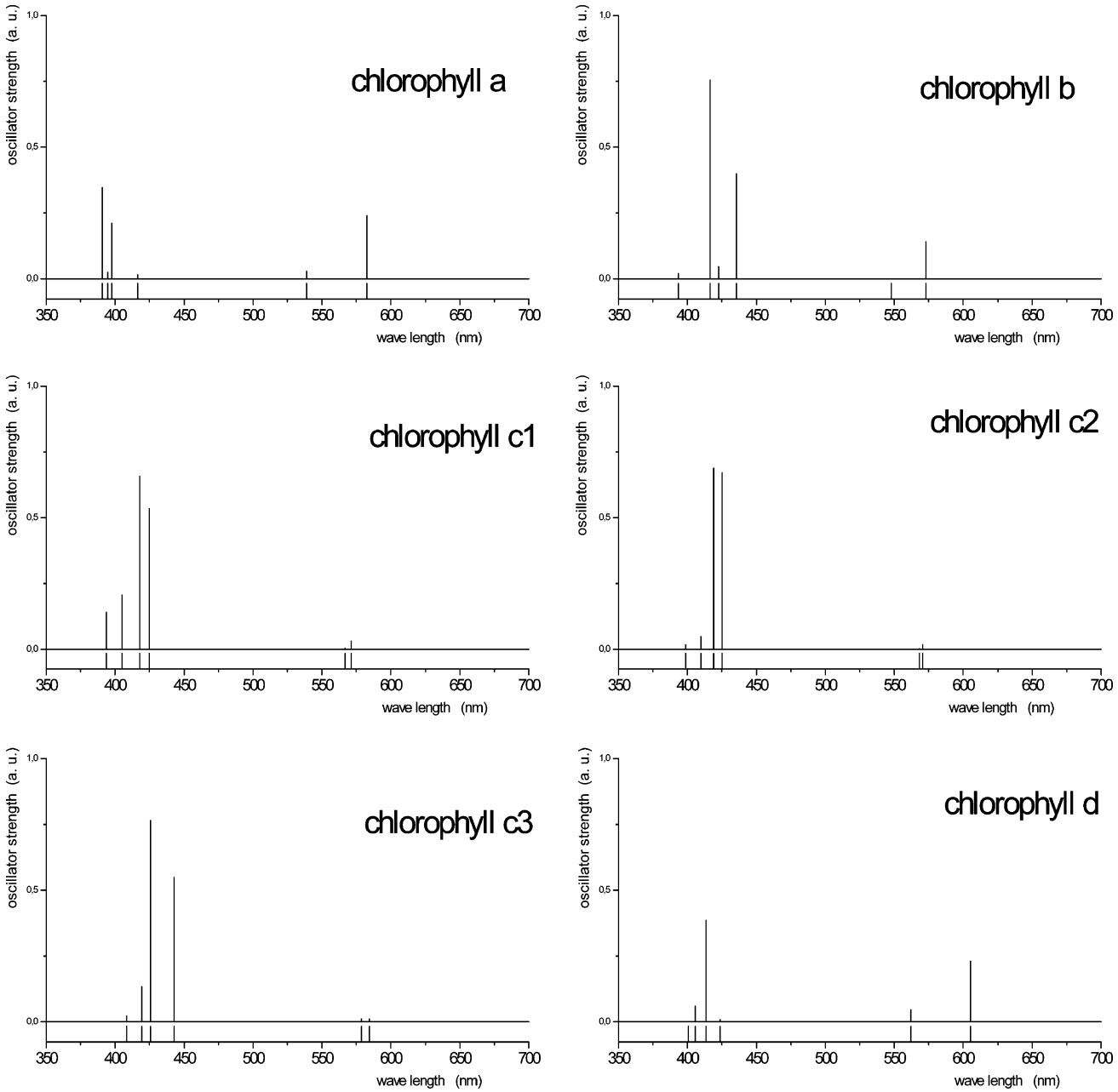

Figure 7. Computed (TDDFT) electron transitions of chlorophyll molecules.

Bacteriochlorophyll *a* is the most abundant chlorophyll-type pigment in the majority of anoxygenic photosynthetic bacteria and its spectrum is well-known (see Figure 12b). The increase of the intensity of the Q bands relative to the Soret band in comparison to the chlorophyll spectrum can be seen in both the measured (Figure 12) and calculated spectra (Figures 7 and 8).

A red shift of the Q_y band of more than 80 nm can be seen when transition energies are compared to the analogous spectra of chlorophyll *a*. Nevertheless, the position of the Soret band is practically the same (or slightly more blue-shifted). In accord with the four-orbital model, the calculated Q band is constituted predominately only by the HOMO → LUMO transition; the contribution from the HOMO − 1 → LUMO + 1 transition is markedly reduced (to the value of about 0.2) in comparison to that in chlorophylls (where this contribution is usually about 0.4). This is due to the increased gap of the unaffected orbital with a_{1u} character and the destabilized (because of the reduced C17−C18 bond) LUMO + 1 with e_{gy} character. A similar destabilization can also be observed in the HOMO with a_{2u} character (compare the energies of the HOMO at −0.188 au for BChl a vs −0.195 au for Chl a). Moreover, the LUMO with e_{gx} character is further stabilized by the presence of the formyl group, as also mentioned in the case of chlorophyll *d*. That is why the Q_y band is so strongly red-shifted.

Bacteriochlorophyll *b* contains an ethylidene (═CH−CH_3) group at the C8 site, which further extends the π-conjugated system (the HOMO energy is further decreased slightly to −0.185 au, preserving the eigenvalues of the other frontier orbitals), resulting in an additional red shift of the Q_y band. This pigment absorbs at the longest wavelength of any known chlorophyll type, i.e., according to our results, at about 700 nm (the experimental value is 794 nm). In comparison to BChl a, the Soret band is accordingly also red-shifted (the edge starts at about 400 nm). The B line is constituted mainly by the HOMO → LUMO + 1 electron transition.

Bacteriochlorophylls *c*−*e* form an "exceptional" group similar to chlorophylls *c*. The porphyrin ring is reduced only partially

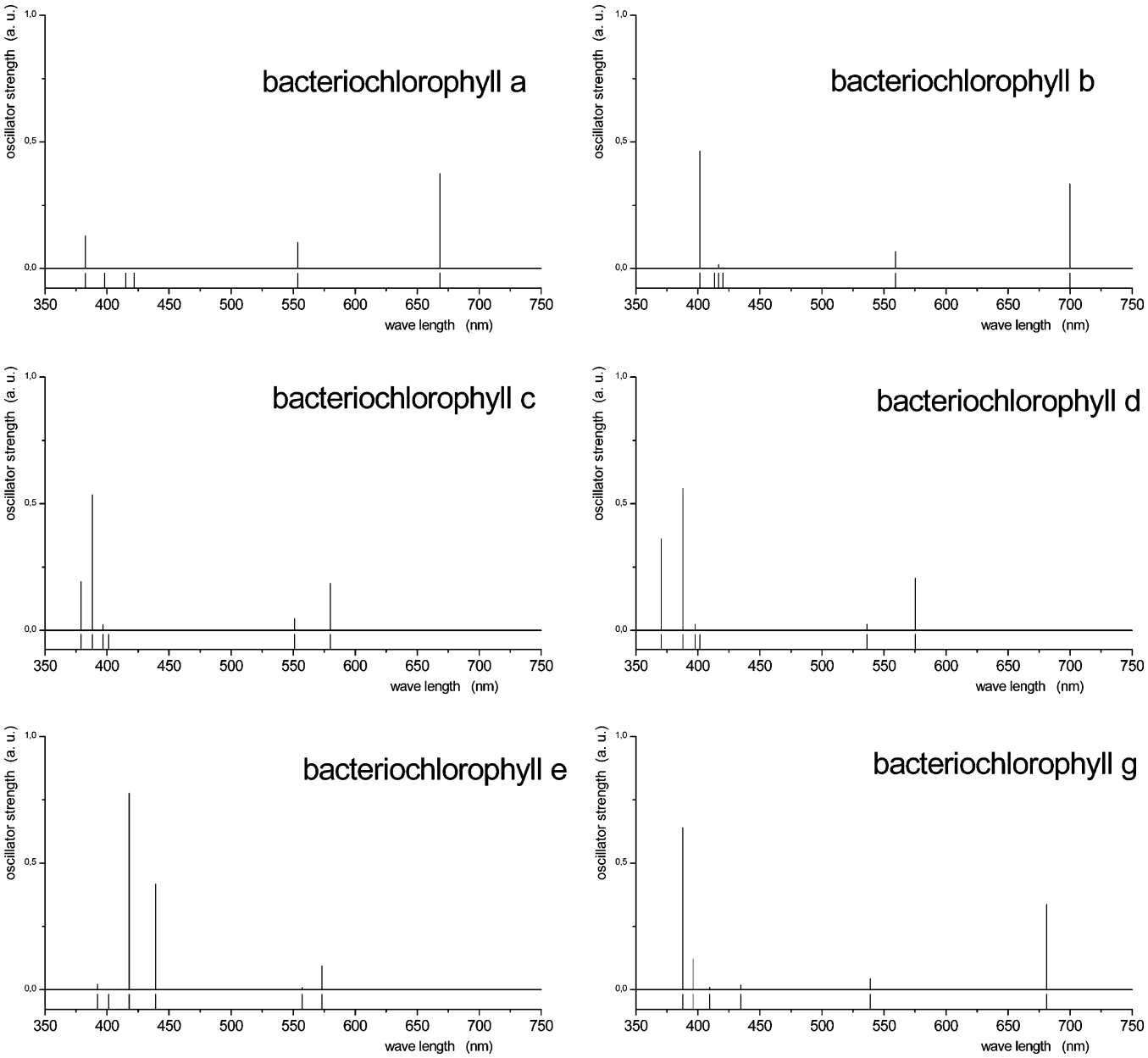

Figure 8. Computed (TDDFT) electron transitions of bacteriochlorophylls.

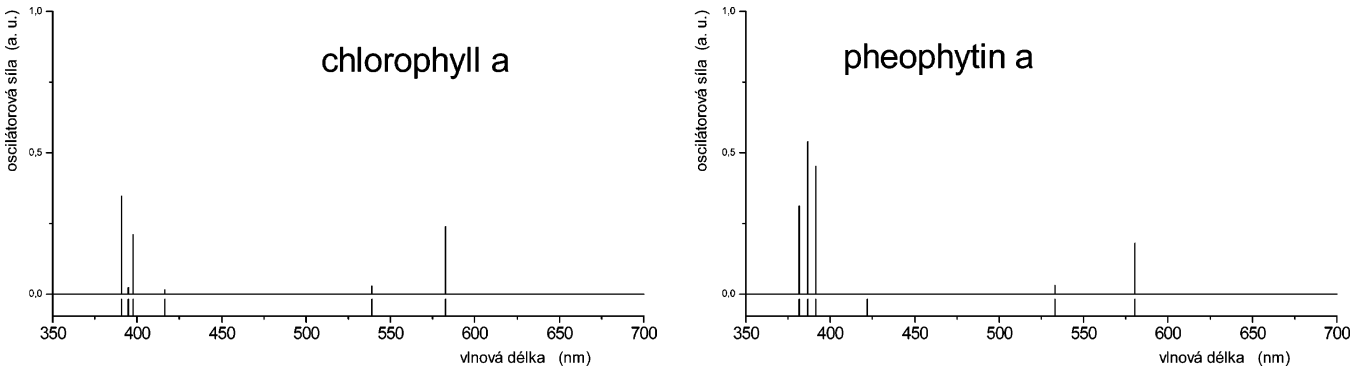

Figure 9. Comparison of calculated electron transitions of chlorophyll *a* and pheophytin *a*.

(C7−C8 bond), in the same way as in chlorophyll systems. Therefore, the structural and spectroscopic characteristics of these bacteriochlorophylls also resemble those of chlorophylls more closely. The Q_y band is positioned just below 580 nm and is composed of both the HOMO → LUMO and HOMO − 1 → LUMO + 1 transitions with weights very similar to those in the electron spectra of chlorophylls. Also, the intensities of the Q bands in relation to the Soret band are substantially lower.

The role of the formyl group in the case of BChl e can be clearly recognized from even more reduced Q_y intensity because the p_z AO of the formyl carbon is visibly present in the HOMO and LUMO + 1 but not the HOMO − 1 and LUMO. Thus, the

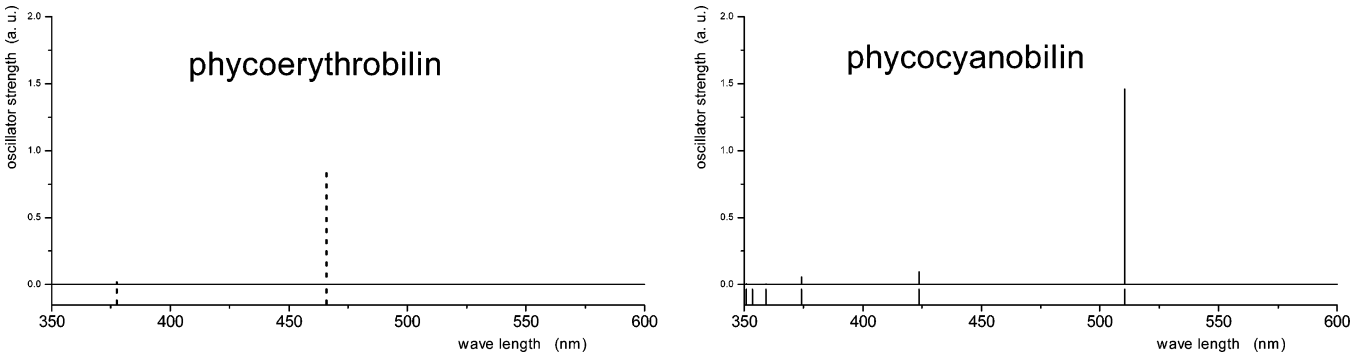

Figure 10. Computed (TDDFT) electron transitions of selected phycobilins. Phycoerythrobilin: dotted lines for the complex with one cysteine molecule and solid lines for the pigment with two cysteine molecules.

overlap of the relevant orbitals in the transition dipole moment formula is decreased. The additional small blue shift of the first transition line is related to a larger stabilization of the HOMO again as a consequence of the incorporation of the formyl p_z AO into the π-conjugated system.

Some changes also occur in the Soret band, which is formed predominately by the HOMO→LUMO + 1 transition. Because the formyl p_z AO is involved in both of these MOs, the intensity of this band is increased accordingly. An apparent shift toward longer wavelength can be noticed. Moreover, at the edge of the Soret band, another transition appears in which the HOMO − 1 → LUMO + 1 transition dominates (its character is based on an inverse combination of the excitation weights of the Q_y line). All of the energies and intensities are in agreement with the experimental data obtained for all three bacteriochlorophylls.[77]

Bacteriochlorophyll *g* has a vinyl group located at the C3 position as in chlorophyll *a*. Moreover, an ethylidene group is present at the C8 site. Bacteriochlorophyll *g* was found to be relatively unstable; it can be easily reduced by saturation of the ethylidene double bond and converted into chlorophyll *a*. In its spectrum, the Q_y band is positioned at about 680 nm with a prevailing HOMO → LUMO transition similar to Q_y of bacteriochlorophyll *a*. Comparing Q_y with the analogous band of chlorophyll *a*, a red shift of about 98 nm can be noticed, in accord with an analogous experimental difference of ca. 105 nm. The edge of the Soret band is also made up of two transitions. In addition to the usual HOMO − 1 → LUMO line (at 388 nm), another less intense line at 396 nm can be observed.

Pheophytin *a*. All chlorophylls and bacteriochlorophylls have their own pheophytin or bacteriopheophytin variants. Structurally, the only difference lies in the absence of the magnesium cation in the center of the porphyrin ring. In this study, the electron spectrum of only the pheophytin *a* molecule was explored for the purpose of comparison with the most common chlorophyll *a*. In Figure 9 and Table 1, the spectrum of pheophytin *a* is presented. The spectra of chlorophyll *a* and pheophytin *a* exhibit prominent similarities. Small but significant differences are in good agreement with analogous differences found in the measured spectra in Figure 12a. The Q transitions are more intense in chlorophyll than in pheophytin. The oscillator strengths for the first and second transitions of chlorophyll are more than 30% larger. Similar results were also published by Hasegawa et al.,[25] Parusel and Grime,[26] and Sundholm.[33] Because the AOs of the magnesium cation are not involved in any of the frontier MOs of the π-conjugated system, the small differences between the chlorophyll and pheophytin spectra can be readily understood. Also, an approximately 2 times larger intensity of the Soret band with respect to the Q_y band was obtained for pheophytin, which is in agreement with the experimental spectra in Figure 12a. Our calculations failed to describe the relative difference of the Q_x position compared to the Q_y band, which is about 30 nm in the measured spectra but less than 10 nm in the TDDFT results (see Table 1).

Phycobilins. These pigments can be characterized by open-chain tetrapyrrole structures covalently bound to proteins (cf. Figure 3). Their structures are very flexible, giving fairly different spectral bands. This feature is partially described in several textbooks, such as ref 78. Therefore, the relevant "biological structures" were taken from the Protein Data Bank.

Phycoerythrobilin and phycocyanobilin were chosen for a study of the influence of structure on spectral properties. The basic difference between these two molecules lies in the chromophore length. Whereas phycoerythrobilin has one saturated bridge (—CH_2—) and two unsaturated bridges (—CH=), phycocyanobilin has all bridges unsaturated. A longer conjugated chromophore chain in phycocyanobilin is clearly visible in the spectral differences between the two molecules (cf. Figure 10 and Table 3), in accordance with the experimental results depicted in Figure 15. However, the unsaturated chromophore chain is far from being planar, and thus, the π-conjugated system is severely perturbed, as can be seen in Figure 16 where the optimized structure of phycoerythrobilin is shown. From Figure 3, another difference can be noticed, namely, the number of bonds to proteins. Whereas phycocyanobilin is attached to the peptide through a single covalent bond, in the case of phycoerythrobilin, both ends are fixed in the protein matrix. However, this fact has no substantial effect on the electronic spectra. We also examined the single-anchoring phycoerythrobilin. It was confirmed that the number of anchoring bonds has no substantial influence on the transition spectrum, as can be seen in Figure 10 and Table 3. The predicted spectral lines are in good agreement with the measured data. The estimated position of the first line is blue-shifted by about 100 nm from the experimental values. Comparing the two phycobilins, the relative positions of spectral lines also agree well with experiment. The first spectral line in phycoerythrobilin is blue-shifted by about 44 nm from the corresponding line of phycocyanobilin, in fairly good accord with the experimental shift of 53 nm. The intensities of these lines are not of great concern because they depend strongly on the structure. Moreover, the effect of the environment is also more important in these molecular systems.

Carotenoids. The common feature of carotenoids is a linear chain with a varying length of unsaturated conjugation. Carotenoids have relatively simple absorption spectra. They usually have three absorption bands corresponding to transfers from the lowest vibration level of the ground state to the three lowest vibration levels of the first excited state.[79] Because the vibration problem was not considered in our study, only the position of the first spectral line can be compared to experimental data.

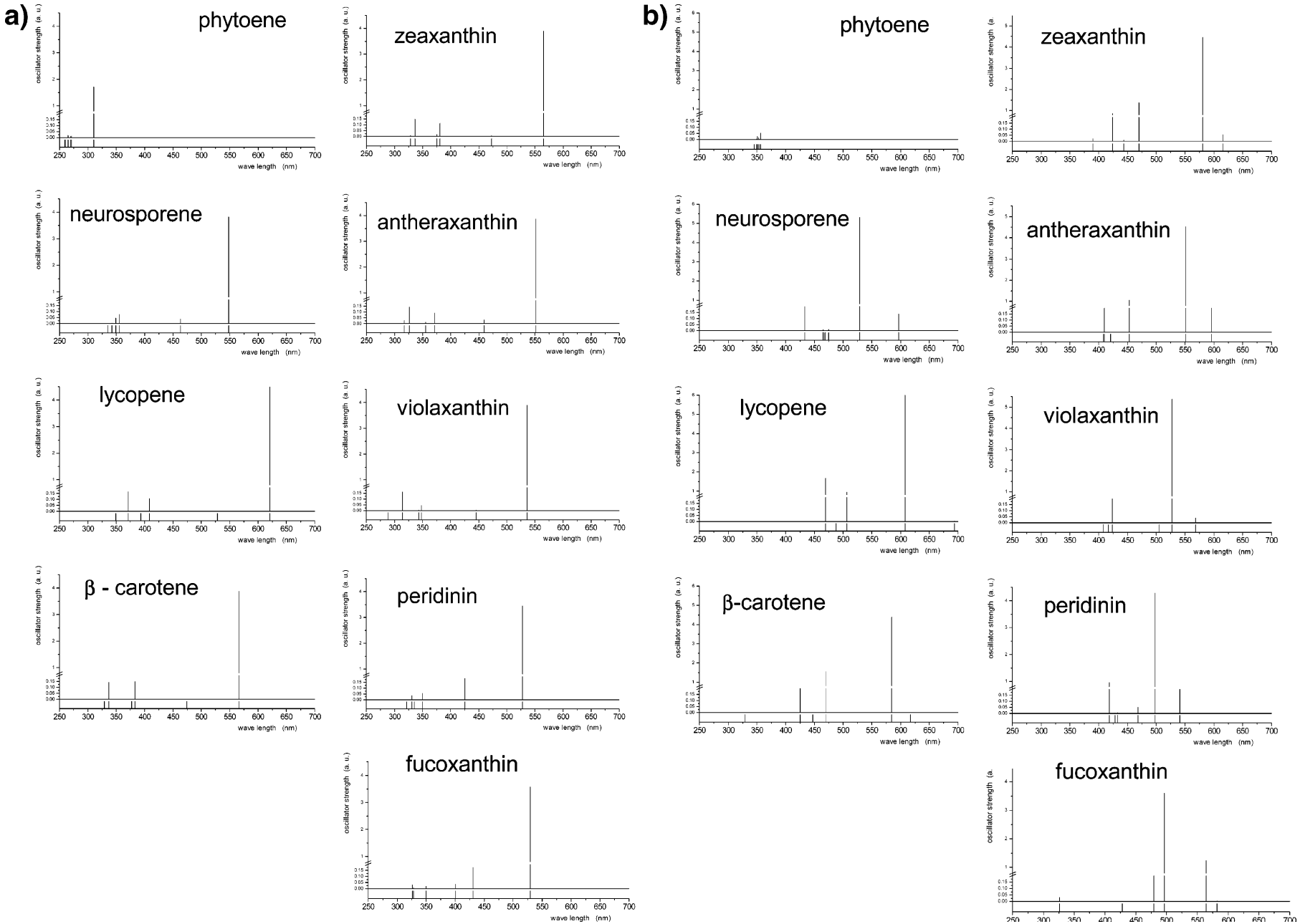

Figure 11. (a) TDDFT and (b) TDA electron transitions of the most frequent carotenoids.

TABLE 1: Experimental Data and Computed (TDDFT) Electron Transitions for Chosen Chlorophyll Structures[a]

Chl a	λ [nm] in diethyl ether	**662**	**578**		**430**		
	λ [nm]	**583**	**539**	**416**	**398**	**395**	**391**
	oscillator strength	*0.24*	*0.03*	*0.02*	*0.21*	*0.03*	*0.35*
Chl b	λ [nm] in diethyl ether	**644**	**549**	**455**			
	λ [nm]	**573**	**548**	**436**	**423**	**417**	**393**
	oscillator strength	*0.14*	*0.*	*0.40*	*0.05*	*0.75*	*0.02*
Chl c1	λ [nm] in diethyl ether	**628**	**578**	**444**			
	λ [nm]	**571**	**567**	**425**	**418**	**405**	**394**
	oscillator strength	*0.03*	*0.*	*0.54*	*0.66*	*0.21*	*0.14*
Chl c2	λ [nm] in diethyl ether	**628**	**579**	**448**			
	λ [nm]	**571**	**568**	**425**	**419**	**410**	**399**
	oscillator strength	*0.02*	*0.*	*0.67*	*0.69*	*0.05*	*0.02*
Chl c3	λ [nm] in diethyl ether	**626**	**586**	**452**			
	λ [nm]	**584**	**579**	**443**	**426**	**419**	**408**
	oscillator strength	*0.01*	*0.01*	*0.55*	*0.77*	*0.13*	*0.02*
Chl d	λ [nm] in diethyl ether	**668**	-		**447**		
	λ [nm]	**605**	**562**	**424**	**413**	**406**	**401**
	oscillator strength	*0.23*	*0.05*	*0.01*	*0.38*	*0.06*	*0.*
Pheo a	λ [nm] in diethyl ether	**672**	**540**		**416**		
	λ [nm]	**580**	**533**	**422**	**391**	**387**	**381**
	oscillator strength	*0.18*	*0.03*	*0.*	*0.45*	*0.54*	*0.31*

[a] Experimental data on gray background taken from Scheer.[2]

TABLE 2: Experimental Data and Computed (TDDFT) Electron Transitions for Bacteriochlorophyll Molecules[a]

BChl a	λ [nm] in diethyl ether	**773**	**577**				**358**
	λ [nm]	**668**	**554**	**422**	**415**	**398**	**383**
	oscillator strength	*0.37*	*0.10*	*0.*	*0.*	*0.*	*0.13*
BChl b	λ [nm] in diethyl ether	**794**	**578**				**368**
	λ [nm]	**700**	**559**	**420**	**417**	**414**	**402**
	oscillator strength	*0.33*	*0.07*	*0.*	*0.02*	*0.*	*0.46*
BChl c	λ [nm] in diethyl ether	**659**	-			**429**	
	λ [nm]	**580**	**551**	**401**	**397**	**388**	**379**
	oscillator strength	*0.19*	*0.05*	*0.*	*0.02*	*0.54*	*0.19*
BChl d	λ [nm] in diethyl ether	**651**				**423**	
	λ [nm]	**575**	**536**	**402**	**398**	**388**	**370**
	oscillator strength	*0.21*	*0.02*	*0.*	*0.03*	*0.56*	*0.36*
BChl e	λ [nm] in diethyl ether	**647**	-	**458**			
	λ [nm]	**573**	**557**	**439**	**418**	**401**	**392**
	oscillator strength	*0.09*	*0.01*	*0.42*	*0.78*	*0.*	*0.02*
BChl g	λ [nm] in diethyl ether	**767**	**565**			**404**	
	λ [nm]	**681**	**539**	**435**	**409**	**396**	**388**
	oscillator strength	*0.34*	*0.04*	*0.02*	*0.01*	*0.12*	*0.64*

[a] Experimental results on gray background taken from Scheer.[2]

TABLE 3: Experimental Data[a] and TDDFT Computed Electron Transitions for Phycobilins

phycocyanobilin	water	**617**	**555**				
	λ [nm]	**510**	**424**	**374**	359	354	351
	oscillator strength	*1.46*	*0.10*	*0.06*	*0.*	*0.*	*0.*
phycoerythrobilin	water	**565**		**495**			
(1AA)	λ [nm]	**466**	390	**377**	348	333	326
	oscillator strength	*0.86*	*0.*	*0.02*	*0.01*	*0.01*	*0.01*
phycoerythrobilin	λ [nm]	**466**	**378**	349	333	332	**326**
(2AA)	oscillator strength	*0.83*	*0.02*	*0.*	*0.02*	*0.*	*0.05*

[a] Results on gray background were taken from the Prozyme *Phycobiliproteins* Web page.[81]

In the computational model, only all-trans isomers were considered. All obtained spectra exhibit a systematic red shift relative to the experimental data that is roughly proportional to the number of unsaturated double bonds. For the reddest line, the shift varies from 13 nm, for phytoene with three double bonds, to 119 nm, for lycopene with a π-conjugated system formed by 11 double bonds. The average shift is about 70 nm. This variation is an unpleasant property and makes the spectral analysis somewhat more complicated than in the previous case of tetrapyrrole systems. Nevertheless, comparing the relative positions of the spectral lines, acceptable agreement with the measured spectra is achieved. The electron transition lines for the complete set of chosen carotenoids are presented in Figure 11 and Table 4. In the TDA spectrum of phytoene, the molecule with the shortest π-conjugated system, some problems can be noticed. Whereas a pronounced intensity for the excitation to S2 state can be seen in the full TDDFT(B3PW91) results, in the results obtained by the TDA method, the intensity of this transition is too low. However, a very similar spectrum was also obtained at the TDDFT(BLYP) level, demonstrating that this particular problem is instead related to the BLYP functional.

TABLE 4: Experimental Data[a] and Computed Electron Transitions at the TDA/TDDFT(BLYP)/6-31+G* and TDDFT(B3PW91)/6-31+G* Levels for Carotenoids

phytoene	λ [nm] in hexan	**297**	**286**	**276**		
TDA	λ [nm]	**356**	354	**352**	**350**	349
	oscillator strength	*0.05*	*0.*	*0.02*	*0.02*	*0.*
full	λ [nm]	**310**	**271**	**269**	**265**	260
	oscillator strength	*1.71*	*0.01*	*0.01*	*0.02*	*0.*
neurosporene	λ [nm] in hexan	**468**	**440**	**415**		
TDA	λ [nm]	*597*	**529**	**475**	468	465
	oscillator strength	*0.14*	*5.31*	*0.01*	*0.*	*0.01*
full	λ [nm]	**548**	**463**	**355**	349	343
	oscillator strength	*3.83*	*0.04*	*0.08*	*0.05*	*0.*
lycopene	λ [nm] in hexan	**502**	**470**	**444**		
TDA	λ [nm]	694	**608**	**506**	488	488
	oscillator strength	*0.01*	*6.07*	*0.94*	*0.*	*0.*
full	λ [nm]	**621**	528	**409**	393	**371**
	oscillator strength	*4.50*	*0.*	*0.11*	*0.*	*0.16*
β-carotene	λ [nm] in hexan	**478**	**450**	**425**		
TDA	λ [nm]	617	**585**	**470**	447	**425**
	oscillator strength	*0.*	*4.38*	*1.54*	*0.*	*0.79*
full	λ [nm]	**566**	474	**383**	377	**337**
	oscillator strength	*3.87*	*0.*	*0.15*	*0.*	*0.14*
zeaxanthin	λ [nm] in ethanol	**478**	**450**	**425**		
TDA	λ [nm]	615	**581**	**470**	444	**424**
	oscillator strength	*0.05*	*4.46*	*1.37*	*0.01*	*0.85*
full	λ [nm]	**565**	473	**381**	375	**336**
	oscillator strength	*3.89*	*0.*	*0.11*	*0.02*	*0.15*
antheraxanthin	λ [nm] in ethanol	**474**	**445**	**422**		
TDA	λ [nm]	*596*	**552**	**453**	421	**410**
	oscillator strength	*0.33*	*4.52*	*1.06*	*0.*	*0.25*
full	λ [nm]	**551**	**459**	**371**	355	**326**
	oscillator strength	*3.85*	*0.08*	*0.09*	*0.01*	*0.14*
violaxanthin	λ [nm] in ethanol	**470**	**440**	**419**		
TDA	λ [nm]	568	**526**	505	**424**	417
	oscillator strength	*0.08*	*5.37*	*0.*	*0.53*	*0.*
full	λ [nm]	**536**	445	**348**	343	**314**
	oscillator strength	*3.89*	*0.01*	*0.05*	*0.*	*0.16*
fucoxanthin	λ [nm] in ethanol	**475**	**449**	**426**		
TDA	λ [nm]	582	***565***	**496**	**479**	428
	oscillator strength	*0.*	*1.24*	*3.59*	*0.71*	*0.*
full	λ [nm]	**529**	**431**	**400**	350	328
	oscillator strength	*3.57*	*0.17*	*0.04*	*0.02*	*0.*
peridinin	λ [nm] in hexan	**485**	**455**			
TDA	λ [nm]	*541*	**498**	**468**	433	429
	oscillator strength	*0.55*	*4.28*	*0.05*	*0.*	*0.*
full	λ [nm]	**528**	**426**	**350**	335	331
	oscillator strength	*3.45*	*0.18*	*0.05*	*0.*	*0.04*

[a] Results on gray background were taken from *Carotenoids.*[79]

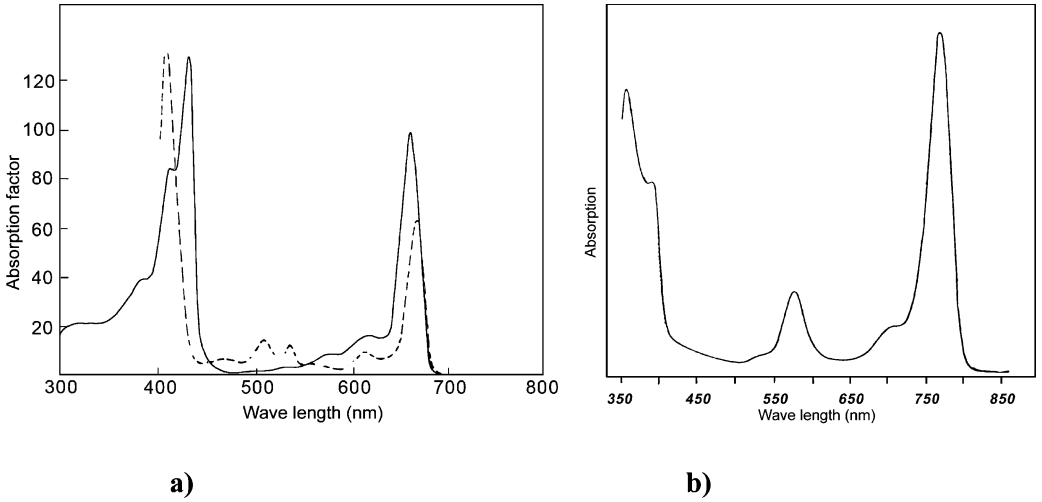

Figure 12. Experimental absorption spectra of (a) chlorophyll *a* (—) and pheophytin *a* (– –) and (b) bacteriochlorophyll *a*. All spectra measured in diethyl ether.[2]

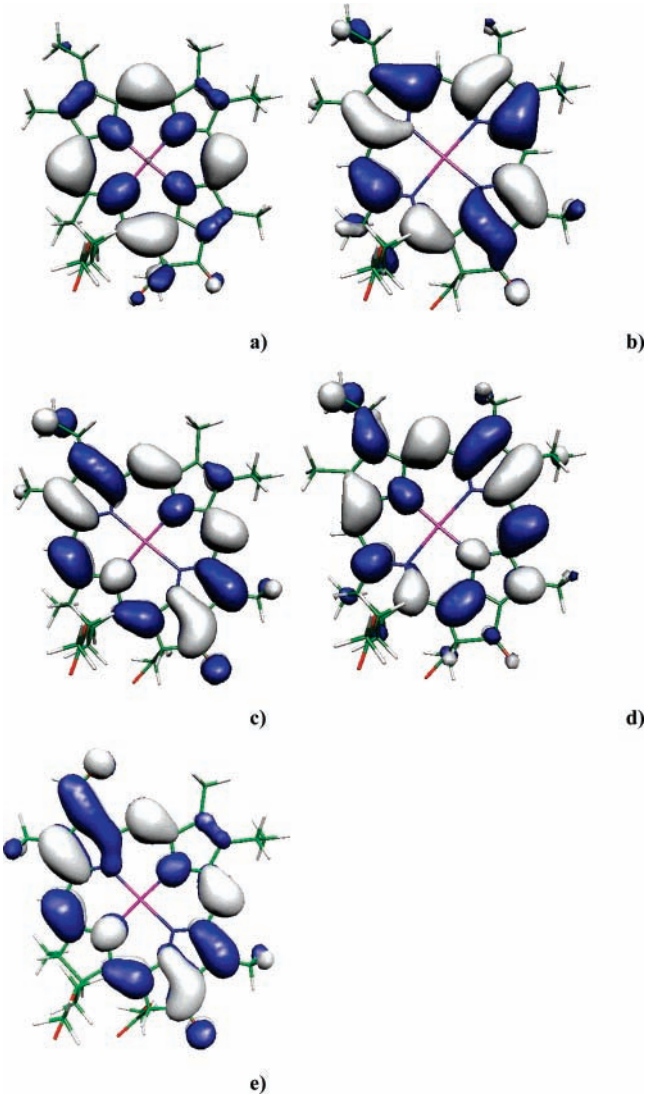

Figure 13. (a–d) Frontier MOs of chlorophyll *a*: MOs from 165 to 168; the 166th MO is the HOMO. (e) LUMO of chlorophyll *d*.

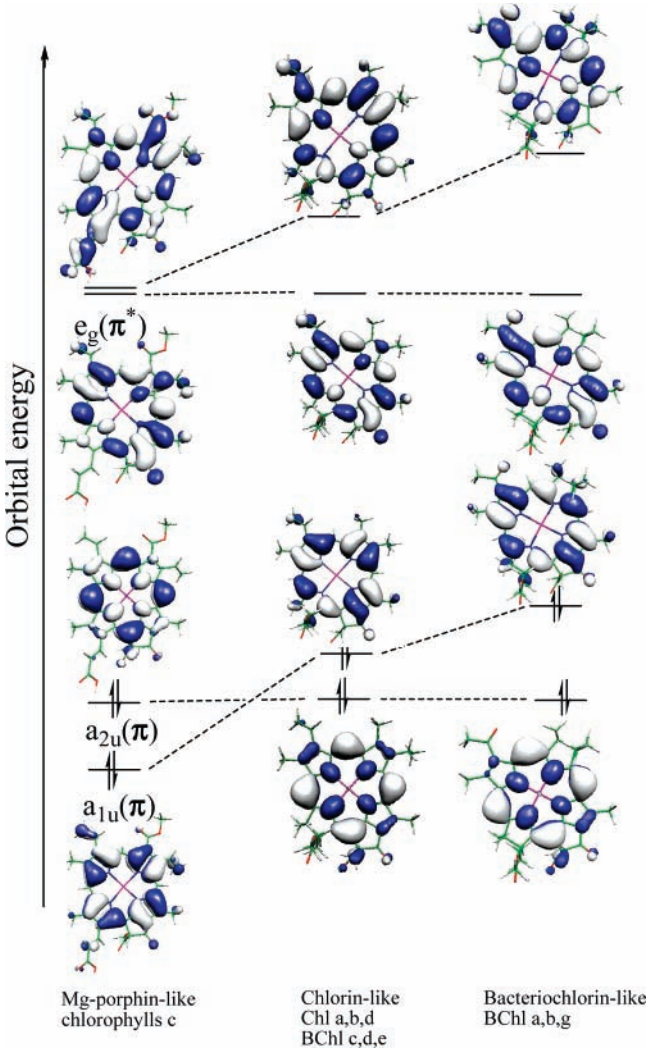

Figure 14. Changes in frontier orbital eigenvalues in going from a free-base porphin such as chlorophyll *c* to bacteriochlorophyll molecules.

S1 and S2 States. In all determined spectra, a remarkably strong absorption (with high intensity) of the first visible transition was found. This line is related to the excitation from the HOMO to the LUMO, which have opposite symmetry according to the classification of unsaturated chains within Hückel theory. According to this concept, "gerade" and "ungerade" MOs alternate regularly. This feature is largely preserved in more accurate calculations as well. Therefore, large transition dipole moments can be expected for the excitation between the HOMO and LUMO, resulting in a high intensity

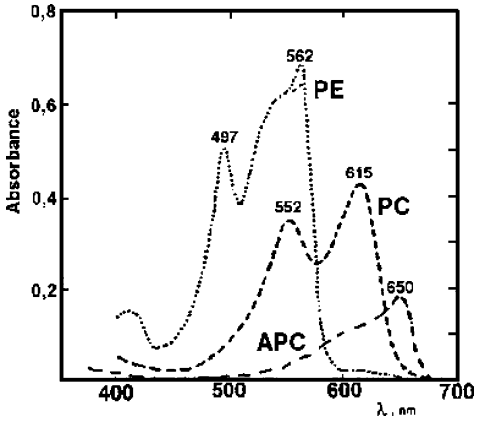

Figure 15. Absorption spectra of phycoerythrobilin (PE), phycocyanobilin (PC), and allophycocyanin (APC).

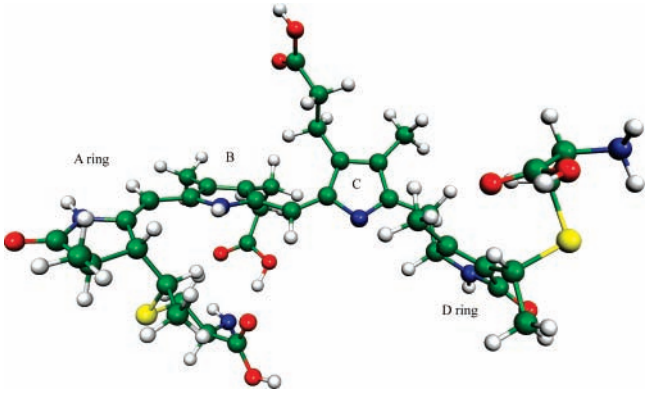

Figure 16. B3PW91/6-31G(d)-optimized structure of phycoerythrobilin anchored to two cysteine molecules.

of this transition. The second singlet $^1B_u^+$ excitation is predicted as the first one at the TDDFT level, whereas the TDA approach correctly inverts the order of the excited states, placing the S1($2^1A_g^-$) excitation at longer wavelengths. The A_g^- line is associated with an electron transition from the HOMO − 1 to the LUMO with some admixture of the HOMO → LUMO + 1 transition. This excitation has a very low intensity (invisible in spectra), which again follows from simple Hückel theory. Because the two MOs have the same gerade symmetry, there is always a very small transition dipole moment between such orbitals. When the character of the unsaturated π-conjugated system is substantially perturbed, as in peridinin, fucoxanthin, and antheraxanthin, an increase in the intensity of this spectral line can be noticed.

Effect of the Chromophore Chain Length. As the chromophore chain elongates, electrons are increasingly delocalized, decreasing the excitation energy. Therefore, the increasing length of the conjugated chain strongly correlates with a longer wavelength for electron transitions in the following order: phytoene, neurosporene, and lycopene, i.e., in carotenoids without any other structural features such as β-cycles. In the case of phytoene, only three conjugated double bonds are present (with the first absorption at about 310 nm at the TDDFT level); neurosporene has nine (about 550 nm) and lycophene has 11 conjugated double bonds (with excitation energy of about 620 nm). Also, the intensity of the line increases with the elongation of the chromophore chain. The extension of the π-conjugated chain by two double bonds causes an increase in the wavelength of about 80 nm. This is slightly larger than the corresponding experimental shift (62 nm). As mentioned above, the length of the conjugated system influences the size of the deviation between the computational and experimental values.

Effect of β-Cycles. Lycopene and β-carotene contain π-conjugated systems of the same length. However, in the carotene molecule, two additional β-cycles are present on the two ends of the linear chain where the edge double bond is incorporated. Comparing the two carotenoids, the effect of the β-cycle can be elucidated. It causes a blue shift of the S2 transition lines from 608 (621) nm according to the TDA (TDDFT) method for lycopene to 585 (566) nm for β-carotene. Similar shifts can be seen for other spectral lines of β-carotene as well. A smaller oscillator strength of this transition is visible in for this molecule. The experimentally observed difference between lycopene and β-carotene in the first absorption peak is practically the same (24 nm) as predicted by the TDA methods. On the other hand, the question of whether β-carotene should still be considered as a system with 11 conjugated double bonds remains in dispute because two of the bonds (one at each end) are involved in β-cycles. Because these cycles deviate from the plane of the π system, they represent a perturbation of the conjugation. Moreover, the spectrum of β-carotene is closer to the spectrum of neurosporene, in terms of not only the frequencies of the lines but also the intensity of the first visible transition.

Effect of the C3 Hydroxyl Group. Another comparison involves zeaxanthin and β-carotene. The zeaxanthin molecule is a derivate of β-carotene in which two hydroxyl groups are located on the C3 carbons of the β-cycles. The experimental spectra of these two pigments are practically identical. This means that hydroxyl groups have no substantial effect on the spectrum. This can be explained by the fact that a hydroxyl group cannot be incorporated into π-electron conjugation. This was also confirmed by the analysis of frontier MOs. Practically no expansion coefficients for the AOs of oxygen were detected within the five highest-occupied and four lowest-energy virtual MOs. The estimated electron transitions are in fairly good accord with the experimental spectra.

Effect of Epoxy Groups and Xanthophyll Cycles. The formation of xantophyll cycles is an important feature present in regulation processes that control the wavelength of light absorption (rather than the intensity). In Figure 11, the blue shift of the S2 transition is visible passing from zeaxanthin through antheraxanthin to violaxanthin. The shift is nearly equidistant in both the experimental and calculated values and originates from the replacement of the double bond present in the β-cycle by an oxygen insertion to form an epoxy group. This causes a shortening of the π-conjugated system by one double bond on each side of the chain. Nevertheless, the change in energy of the first allowed transition (S2), about 25 (15) nm by TDA (TDDFT), is not fully comparable to the above-discussed effect of the length of the chromophore chain because these double bonds are already involved in β-cycles. Nevertheless, the computed energy differences for transition to the S2 state between the three xanthines are still substantially larger than the corresponding experimental values as a consequence of the overestimated dependence of the transition lines on the length of the π-conjugated system (as mentioned above). The intensity of the S2 transition increases during the epoxidation from zeaxanthin to violaxanthin at the TDA level, in contrast to the TDDFT results, according to which the intensity remains practically constant. The red shift of the S2 spectral line, going from violaxanthin to zeaxanthin, could be related to the possibility of starting a nonphotochemical quenching (NPQ) mechanism, expecting that the de-epoxidazed zeaxanthin forms an "energy sink" as suggested in ref 1. However, another

possibility of NPQ should be stressed. The TDA results exhibit a larger difference between the S1 and S2 states in the violaxanthin spectrum (about 60 nm) than in the zeaxanthin spectrum, where only a 40 nm gap was found. This means that, in zeaxanthin, the S1 and S2 energy levels are substantially closer, which can clearly play a key role in NPQ mechanism.

Effect of Other Groups. Peridinin and fucoxanthin can be used to elucidate another structural feature of carotenoids. Both contain the allenic group (−CH═C═CH−). The presence of this group plays an important role in plants such as algae that do not contain chlorophyll *b* in their antenna complexes. In addition, fucoxanthin contains one carbonyl group at the C8 position, and peridinin contains a lactone group near the C8 position, which makes the analysis of various structural groups more complicated. The carbonyl group together with the allenic moiety makes the spectrum slightly red-shifted compared to the spectrum of violaxanthin. From Table 4, it can be seen that the experimental red shift of 5 nm qualitatively differs from the computed blue shift of 7 nm (using the TDDFT method) or 30 nm (at the TDA level). However, it can be guessed that the relative error in the estimation of spectral lines is more than 10 nm. In the TDA-predicted spectra, another state ($1^1B_u^-$) was localized between $1^1B_u^+$ and $2^1A_g^-$. This state is mainly made up of the HOMO − 2 → LUMO transition and lies slightly higher in other carotenoids.

The experimental spectral bands of peridinin are slightly red-shifted in comparison to the corresponding bands of fucoxanthin (by about 10 nm). The calculated results obtained by TDA match this trend well. From the comparison of the similar spectra of fucoxanthin and peridinin, the superior performance of TDA over the full TDDFT method is apparent in this particular case of carotenoids. Some additional support for the better performance of TDA can be also seen in the work of Dreuw et al. on increasing the length of polyene chains, in which results from more sophisticated ADC(2) (algebraic diagrammatic constructions to the second order) are compared.[74] The TDDFT results do not reproduce the relative positions of peridinin spectral lines, whereas the TDA approach fits the experimental values substantially better.

Error Estimation of the Electron Transitions. The predicted first spectral lines of (bacterio)chlorophyll and phycobilin molecules are usually shifted by up to 100 nm toward longer wavelengths in comparison to the experimental results. Smaller differences can be seen for higher excitation energies. In the blue region, the error usually drops to below 40 nm. The differences between measured and computed lines vary for every group of pigments. However, the effect caused by various ligands within a group of pigments is easily visible. It can be mentioned that the error in the spectral line determination is inherent in the chosen method, basis set, and system (here, π-conjugated systems of tetrapyrrole structures with similar sizes) and is therefore practically constant for these particular pigment groups. Another source of deviations between experimental spectra and calculated lines is related to different environments or surrounding molecules. Our calculations at this stage were performed for the in vacuo model. Considering these aspects, a very good accuracy (small relative error for the each given spectral line) with experimental data was achieved for the TDDFT(B3LYP) method and the chosen basis set.

In contrast to chlorophyll/phycobilin systems, the determination of the electron absorption spectra of carotenoids is related to a fundamental problem. That is, the error in spectra determination is dependent on the examined systems and exhibits a dependence on the size of the π-conjugated system, as mentioned above. Therefore, it is more difficult to estimate even relative positions of various spectral lines.

Conclusion

In this study, various pigments from photosystems were explored. The most stable conformations were chosen based on a database search, with subsequent geometry optimization performed in several steps at different computational levels.

For the global minima, electronic excitations were determined using the TDDFT method at the B3PW91/6-31+G(d) level. For the group of carotenoids, the TDA approach with the non-hybrid BLYP functional and the same basis set was compared.

In the spectra of chlorophylls and pheophytin transition lines, lower intensities were determined for the Q bands than for the Soret band. Spectral energies of the Q_y lines were systematically blue-shifted by about 50−80 nm. Nevertheless, the correct order of these Q lines among various chlorophyll types can be noticed from a comparison with experimental results. A much better agreement was obtained for the edge of the Soret band represented by B transitions, for which the difference was at most 35 nm in the case of chlorophyll *d*.

Similar conclusions also hold for bacteriochlorophylls. The Q_y line is slightly more shifted, on average, in comparison to the experimental transition—by about 85 nm. For the bacteriochlorophylls, a correct higher intensity of the Q_y band compared to the Soret band was obtained.

In the case of phycobilins, the large flexibility of the open tetrapyrrole system can lead to quite artificial electron transitions. Therefore, obtaining the proper molecular conformation from the structural database was very important. The first transition line of phycobilins occurs at substantially lower wavelengths (by around 500 nm) and has a dominant character (high intensity). The influence of anchoring a cysteine side chain was found to be relatively small.

Spectral lines of carotenoids are based on linear polyene chains, which have a dominant influence on the spectra. Nevertheless, other structural elements such as β-cycles and epoxy, carbonyl, and allenic groups were also investigated. It was found that the first allowed excitation to the S2($1^1B_u^+$) state has a very high intensity because of the different characters of the HOMO and LUMO. According to simple Hückel theory, the even and odd characters of the MOs alternate. Therefore, a large transition dipole moment can be expected for this spectral line. In contrast, the transition to S1($2^1A_g^-$) is, according to the same arguments, forbidden. Because simple Hückel theory is not completely valid (carotenoids do not exhibit the symmetry of the simplified polyene model), some small intensities can be noticed. The largest values appear in the cases of peridinin, fucoxanthin, and antheraxanthin, where the influence of allenic and xantophyll groups is notable.

In the case of fucoxanthin, the $1^1B_u^-$ state was found to lie between the 2^1Ag and 1^1Bu^+ states; it usually lies above this state in the other investigated carotenoinds.

In contrast to the first visible transition lines of chlorophyll molecules, in the case of carotenoids, the S2 transition lines are overestimated (red-shifted) by about 70 nm on average. Nevertheless, because various groups influence the electron transitions to different extents, the error in spectral determination is relatively larger, and so, this red shift varies markedly between individual caroteniod molecules. Recently, an experimental study on the solvent effects of carotenoid spectra was reported in which shorter wavelengths should be expected for transitions in environment with dielectric constant $\epsilon = 1$.[80]

Acknowledgment. This study was supported by grant MSM 0021620835. The Charles University Meta-Centrum in Prague, Czech Republic, is acknowledged for access to its excellent supercomputer facilities. The authors are very grateful to Prof. Tomáš Polívka from South Bohemian University and Profs. Jan Hála and Jakub Pšenčík from our department for very fruitful discussions.

References and Notes

(1) Blankenship, R. E. *Molecular Mechanisms of Photosynthesis*; Blackwell Science Ltd.: Oxford, U.K., 2002.
(2) Scheer, H. *Chlorophylls*; CRC Press: Boca Raton, FL, 1991.
(3) *The Porphyrin Handbook*; Kadish, K. M., Smith, K. M., Guilard, R., Eds.; Academic Press: New York, 2003.
(4) Gouterman, M. *J. Chem. Phys.* **1959**, *30*, 1139.
(5) Gouterman, M.; Wagniere, G. H. *J. Mol. Spectrosc.* **1963**, *11*, 108.
(6) Zerner, M.; Gouterman, M. *Theor. Chim. Acta* **1966**, *4*, 44.
(7) Almlof, J.; Fischer, T. H.; Gassman, P. G.; Ghosh, A.; Haser, M. *J. Phys. Chem.* **1993**, *97*, 10964.
(8) Baraldi, I.; Carnevali, A.; Ponterini, G.; Vanossi, D. *J. Mol. Struct. (THEOCHEM)* **1995**, *333*, 121.
(9) Cortina, H.; Senent, M. L.; Smeyers, Y. G. *J. Phys. Chem. A* **2003**, *107*, 8968.
(10) Gwaltney, S. R.; Bartlett, R. J. *J. Chem. Phys.* **1998**, *108*, 6790.
(11) Hasegawa, J.; Ohkawa, K.; Nakatsuji, H. *J. Phys. Chem. B* **1998**, *102*, 10410.
(12) Hashimoto, T.; Choe, E.; Nakano, H.; Hirao, K. *J. Phys. Chem. A* **1999**, *103*, 1894.
(13) Kitao, O.; Ushiyama, H.; Miura, N. *J. Chem. Phys.* **1999**, *110*, 2936.
(14) Lamoen, D.; Parrinello, M. *Chem. Phys. Lett.* **1996**, *248*, 309.
(15) Merchan, M.; Orti, E.; Roos, B. *Chem. Phys. Lett.* **1994**, *221*, 136.
(16) Merchan, M.; Orti, E.; Roos, B. *Chem. Phys. Lett.* **1994**, *226*, 27.
(17) Serrano-Andres, L.; Merchan, M.; Rubio, M.; Roos, B. O. *Chem. Phys. Lett.* **1998**, *295*, 195.
(18) Nagashima, U.; Takada, T.; Ohno, K. *J. Chem. Phys.* **1986**, *85*, 4524.
(19) Nakatsuji, H.; Hasegawa, J.-Y.; Hada, M. *J. Chem. Phys.* **1996**, *104*, 2321.
(20) Parusel, A.; Grime, S. *J. Porphyrins Phthalocyanines* **2001**, *5*, 225.
(21) Rubio, M.; Roos, B.; Serrano-Andres, L.; Merchan, M. *J. Chem. Phys.* **1999**, *110*, 7202.
(22) Tokita, Y.; Hasegawa, J.; Nakatsuji, H. *J. Phys. Chem. A* **1998**, *102*, 1843.
(23) Sundholm, D. *Phys. Chem. Chem. Phys.* **2000**, *2*, 2275.
(24) Sundholm, D. *Chem. Phys. Lett.* **2000**, *317*, 392.
(25) Hasegawa, J.; Ozeki, Y.; Ohkawa, K.; Nakatsuji, H. *J. Phys. Chem. B* **1998**, *102*, 1320.
(26) Parusel, A. B. J.; Grimme, S. *J. Phys. Chem. B* **2000**, *104*, 5395.
(27) Jeong, D. H.; Jang, S. M.; Hwang, I.-W.; Kim, D.; Yoshida, N.; Osuka, A. *J. Phys. Chem. A* **2002**, *106*, 11054.
(28) Linnanto, J.; Korppi-Tommola, J. *J. Phys. Chem. A* **2000**, *105*, 3855.
(29) Linnanto, J.; Korppi-Tommola, J. *Phys. Chem. Chem. Phys.* **2000**, *2*, 4962.
(30) Linnanto, J.; Oksanen, J. A. I.; Korppi-Tommola, J. *Phys. Chem. Chem. Phys.* **2002**, *4*, 3061.
(31) Linnanto, J.; Korppi-Tommola, J. E. I. *Phys. Chem. Chem. Phys.* **2002**, *4*, 3453.
(32) Cory, M. G.; Zerner, M. C.; Hu, X.; Schulten, K. *J. Phys. Chem. B* **1998**, *102*, 7640.
(33) Sundholm, D. *Chem. Phys. Lett.* **1999**, *302*, 480.
(34) Sundholm, D. *Phys. Chem. Chem. Phys.* **2003**, *5*, 4265.
(35) Edwards, L.; Dolphin, D. H.; Gouterman, M. *J. Mol. Spectrosc.* **1970**, *35*, 90.
(36) Edwards, L.; Dolphin, D. H.; Gouterman, M.; Adler, A. D. *J. Mol. Spectrosc.* **1971**, *38*, 16.
(37) Houssier, Sauer. *J. Am. Chem. Soc.* **1970**, *92*, 779.
(38) Konermann, L.; Gatzen, G.; Holzwarth, A. R. *J. Phys. Chem. B* **1997**, *101*, 2933.
(39) Konermann, L.; Holzwarth, A. R. *Biochemistry* **1996**, *35*, 829.
(40) Doust, A. B.; Marai, C. N. J.; Harrop, S. J.; Wilk, K. E.; Curmi, P. M. G.; Scholes, G. D. *J. Mol. Biol.* **2004**, *344*, 135.
(41) McConnell, M. D.; Koop, R.; Vasil'ev, S.; Bruce, D. *Plant Physiol.* **2002**, *130*, 1201.
(42) Hashimoto, H.; Yoda, T.; Kobayashi, T.; Young, A. J. *J. Mol. Struct.* **2002**, *604*, 125.
(43) Wang, Y. L.; Mao, L. S.; Hu, X. C. *Biophys. J.* **2004**, *86*, 3097.
(44) Garavelli, M.; Bernardi, F.; Olivucci, M.; Robb, M. A. *J. Am. Chem. Soc.* **1998**, *120*, 10210.
(45) He, Z.; Sundstrom, V.; Pullerits, T. *Chem. Phys. Lett.* **2001**, *334*, 159.
(46) Qian, P.; Mizoguchi, T.; Fujii, R.; Hara, K. *J. Chem. Inf. Comput. Sci.* **2002**, *42*, 1311.
(47) Scholes, G. D.; Harcourt, R. D.; Fleming, G. R. *J. Phys. Chem. B* **1997**, *101*, 7302.
(48) Krueger, B. P.; Scholes, G. D.; Fleming, G. R. *J. Phys. Chem. B* **1998**, *102*, 5378.
(49) Krueger, B. P.; Scholes, G. D.; Yu, J. Y.; Fleming, G. R. *Acta Phys. Pol. A* **1999**, *95*, 63.
(50) Krueger, B. P.; Yom, J.; Walla, P. J.; Fleming, G. R. *Chem. Phys. Lett.* **1999**, *310*, 57.
(51) Scholes, G. D.; Fleming, G. R. *J. Phys. Chem. B* **2000**, *104*, 1854.
(52) Walla, P. J.; Yom, J.; Krueger, B. P.; Fleming, G. R. *J. Phys. Chem. B* **2000**, *104*, 4799.
(53) Gradinaru, C. C.; Kennis, J. T. M.; Papagiannakis, E.; van Stokkum, I. H. M.; Cogdell, R. J.; Fleming, G. R.; Niederman, R. A.; van Grondelle, R. *Proc. Natl. Acad. Sci. U.S.A.* **2001**, *98*, 2364.
(54) Hsu, C. P.; Walla, P. J.; Head-Gordon, M.; Fleming, G. R. *J. Phys. Chem. B* **2001**, *105*, 11016.
(55) Kennis, J. T. M.; Gobets, B.; van Stokkum, I. H. M.; Dekker, J. P.; van Grondelle, R.; Fleming, G. R. *J. Phys. Chem. B* **2001**, *105*, 4485.
(56) Walla, P. J.; Linden, P. A.; Ohta, K.; Fleming, G. R. *J. Phys. Chem. A* **2002**, *106*, 1909.
(57) Zimmermann, J.; Linden, P. A.; Vaswani, H. M.; Hiller, R. G.; Fleming, G. R. *J. Phys. Chem. B* **2002**, *106*, 9418.
(58) Holt, N. E.; Kennis, J. T. M.; Dall'Osto, L.; Bassi, R.; Fleming, G. R. *Chem. Phys. Lett.* **2003**, *379*, 305.
(59) Ma, Y. Z.; Holt, N. E.; Li, X. P.; Niyogi, K. K.; Fleming, G. R. *Proc. Natl. Acad. Sci. U.S.A.* **2003**, *100*, 4377.
(60) Vaswani, H. M.; Holt, N. E.; Fleming, G. R. *Pure Appl. Chem.* **2005**, *77*, 925.
(61) You, Z. Q.; Hsu, C. P.; Fleming, G. R. *J. Chem. Phys.* **2006**, *124*, 044506.
(62) Hsu, C. P.; Head-Gordon, M.; Fleming, G. R. *Abstr. Pap. Am. Chem. Soc.* **2000**, *219*, U329.
(63) Dreuw, A.; Fleming, G. R.; Head-Gordon, M. *J. Phys. Chem. B* **2003**, *107*, 6500.
(64) Dreuw, A.; Fleming, G. R.; Head-Gordon, M. *Biochem. Soc. Trans.* **2005**, *33*, 858.
(65) Hirata, S.; Head-Gordon, M. *Chem. Phys. Lett.* **1999**, *314*, 291.
(66) Dreuw, A.; Head-Gordon, M. *J. Am. Chem. Soc.* **2004**, *126*, 4007.
(67) Cai, Z.-L.; Crossley, M. J.; Reimers, J. R.; Kobayashi, R.; Amos, R. D. *J. Phys. Chem. B* **2006**, *110*, 15624.
(68) *Protein Data Bank*; Research Collaboratory for Structural Bioinformatics (RCSB): Piscataway, NJ; http://www.rcsb.org/pdb/home/home.do.
(69) Sundholm, D. *Chem. Phys. Lett.* **2000**, *317*, 545.
(70) Šeda, J.; Burda, J. V.; Leszczynski, J. *J. Comput.Chem.* **2005**, *26*, 294.
(71) Burda, J. V.; Šeda, J.; Brázdová, V.; Kapsa, V. *Int. J. Mol. Sci.* **2004**, *5*, 196.
(72) Chiang, S.-Y.; Lin, I.-F. *J. Chem. Phys.* **2005**, *122*, 094301.
(73) Chong, D. P.; Takahata, Y. *Chem. Phys. Lett.* **2006**, *418*, 286.
(74) Starcke, J. H.; Wormit, M.; Schirmer, J.; Dreuw, A. *Chem. Phys.* **2006**, *329*, 39.
(75) Dreuw, A. *ChemPhysChem* **2006**, *7*, 2259.
(76) Shao, Y.; Fusti-Molnar, L.; Jung, Y.; Kussmann, J.; Ochsenfeld, C.; Brown, S. T.; Gilbert, A. T. B.; Slipchenko, L. V.; Levchenko, S. V.; O'Neill, D. P.; Distasio, R. A., Jr.; Lochan, R. C.; Wang, T.; Beran, G. J. O.; Besley, N. A.; Herbert, J. M.; Lin, C. Y.; Van Voorhis, T.; Chien, S. H.; Sodt, A.; Steele, R. P.; Rassolov, V. A.; Maslen, P. E.; Korambath, P. P.; Adamson, R. D.; Austin, B.; Baker, J.; Byrd, E. F. C.; Dachsel, H.; Doerksen, R. J.; Dreuw, A.; Dunietz, B. D.; Dutoi, A. D.; Furlani, T. R.; Gwaltney, S. R.; Heyden, A.; Hirata, S.; Hsu, C.-P.; Kedziora, G.; Khalliulin, R. Z.; Klunzinger, P.; Lee, A. M.; Lee, M. S.; Liang, W.; Lotan, I.; Nair, N.; Peters, B.; Proynov, E. I.; Pieniazek, P. A.; Rhee, Y. M.; Ritchie, J.; Rosta, E.; Sherrill, C. D.; Simmonett, A. C.; Subotnik, J. E.; Woodcock, H. L., III; Zhang, W.; Bell, A. T.; Chakraborty, A. K.; Chipman, D. M.; Keil, F. J.; Warshel, A.; Hehre, W. J.; Schaefer, H. F., III; Kong, J.; Krylov, A. I.; Gill, P. M. W.; Head-Gordon, M. *Phys. Chem. Chem. Phys.* **2006**, *8*, 3172.
(77) Hoff, A. J.; Amesz, J. Visible Absorption Spectroscopy of Chlorophylls. In *Chlorophylls*; Scheer, H., Ed.; CRC Press: Boca Raton, FL, 1991; pp 723−738.
(78) Hála, J.; Šetlík, J. *Biofyzika Fotosyntézy (Scriptum)*; Carolinum Press: Prague, 1999.
(79) Kohler, E. B. *Carotenoids*; Birkhäuser Verlag: Basel, Switzerland, 1995; Vol. 1B: Spectroscopy.
(80) Chen, Z.; Lee, C.; Lenzer, T.; Oum, K. *J. Phys. Chem. A* **2006**, *110*, 11291.
(81) *Phycobiliproteins*; Prozyme: San Leandro, CA, 1999; http://www.prozyme.com/technical/pbvrwdata.html.